

## Supercapacitor Applications of Polyaniline and Poly(*N*-methylaniline) Coated Pencil Graphite Electrode

Andaç Arslan, Evrim Hür\*

Department of Chemistry, Faculty of Arts and Science, Eskişehir Osmangazi University, 26480 Eskişehir, Turkey

\*E-mail: [evrimhur@ogu.edu.tr](mailto:evrimhur@ogu.edu.tr)

*Received:* 17 October 2012 / *Accepted:* 12 November 2012 / *Published:* 1 December 2012

---

Polyaniline (PANi) and poly(*N*-methylaniline) (PNMA) films have been successfully synthesized on pencil graphite electrode (PGE) using cyclic voltammetry (CV) from acetonitrile (ACN) solution of 0.1 M tetraethylammonium tetrafluoroborate (TEABF<sub>4</sub>) and 0.1 M monomer. These polymers have been characterized by scanning electron microscopy (SEM), CV and Mott-Schottky (MS) analysis. The electrochemical storage properties of PGE coated with PANi (PGE/PANi) and PNMA (PGE/PNMA) have been evaluated using CV, potentiostatic electrochemical impedance spectroscopy (EIS) and charge-discharge measurement. In addition, the voltage range has been determined. By this way, it is suggested for which kind of technological devices supercapacitor can be used as a circuit element. CV and potentiostatic EIS show that the specific capacitance of the PGE/PNMA is higher than the PGE/PANi. On the other hand, according to charge-discharge tests, the PGE/PNMA has better charge-discharge stability than the PGE/PANi.

---

**Keywords:** Polyaniline, Electroactive polymer, Supercapacitor.

### 1. INTRODUCTION

Supercapacitors, also called ultracapacitors or electrochemical capacitors, are important energy storage devices having higher energy density and higher power density compared to batteries and conventional capacitors, respectively [1-3]. They differ from other energy storage devices in their special energy storage process, including faradaic process and capacitive process, lead to their significantly improved energy density and power density [4-6]. Depending on the charge storage mechanism, supercapacitors can be classified in two categories. The electrical double layer capacitor utilizes mainly the separation of the electronic and ionic charges at the interface between electrode

materials and the electrolyte solution [6,7]. Another type of supercapacitor, referred to as a pseudocapacitor, provides its capacitance from faradaic redox reactions occurring within the active materials of electrode [8,9]. Supercapacitors can store and release energy based on single process or both processes, depending on the nature of electrode active materials [10]. Therefore, electrode active materials play an important role in the performance of supercapacitors. Carbon materials such as carbon nanotubes, active carbon and graphite with high surface area have been widely investigated as electrical double layer capacitors [11]. The typical electrode active materials based on pseudocapacitor are transition metal oxides and electrically conducting polymers [12,13]. Among these, as an ideal candidate for pseudocapacitor electrode, electrically conducting polymers are attractive, due to their good electrical conductivities, electrochemical reversibility, fast switching properties, low toxicities and low costs (compared with the relatively expensive transition metal oxides) [14,15]. While carbon materials have a long cycle life, the poor energy storage capacity and limiting rate capability of carbonaceous materials restrict their applications [10]. On the other hand, the disadvantages of electrically conducting polymers include a lower cycle life in charge-discharge than carbonaceous materials because the redox sites in the polymer backbone are not sufficiently stable for many repeated redox processes [16-18]. Therefore, more and more intensive efforts have been devoted to develop supercapacitor electrode active materials which can combine the advantages of both electrical double layer capacitor and pseudocapacitor. Such supercapacitors have demonstrated improvement in the electrical performance [19,20].

Renewable PGE are more preferable materials than other carbonaceous materials because of their low costs and disposable properties and they have been available as writing tools for many years. They don't require cleaning processing. Therefore, creating a new surface of electrode is easy and fast and reproducibility of these electrodes is high. On the other hand, PANi and its derivatives have been considered promising materials in energy storage applications [21-23], and are used in supercapacitor as electrode active materials with high faradaic pseudocapacitance [24] due to the existence of several oxidation structures [25].

In this study, PANi and PNMA were firstly synthesized on PGE using cyclic CV in ACN solution. Secondly, electrochemical characterizations of the obtained polymers were done using CV and MS methods and the surface morphologies of the PGE/PANi and the PGE/PNMA were characterized by SEM. Thirdly, to investigate the ability of these electrodes to serve as supercapacitor electrode active material, electrochemical storage properties of these electrodes were examined. Thus, CV and potentiostatic EIS were used to calculate capacitance ( $C$ , F), the area-specific capacitance ( $C_{as}$ ,  $\text{Fcm}^{-2}$ ) and the mass-specific capacitance ( $C_{ms}$ ,  $\text{Fg}^{-1}$ ). In the real applications, the  $C_{as}$  is a better indicator of the performance of supercapacitor, although the  $C_{ms}$  have always been used in the literature for comparison of the performance of supercapacitor [26]. The cycle durabilities and voltage ranges of these electrodes were determined using repeating chronopotentiometry (RCP) method. There is no report in available literature dealing with the direct deposition PANi and PNMA on PGE from ACN solution and availability as supercapacitor electrode active materials of the PGE/PANi and the PGE/PNMA. Therefore we are investigating possibility of utilizing the PGE/PANi and the PGE/PNMA as alternative to other investigated materials for supercapacitor applications.

## 2. EXPERIMENTAL

### 2.1. Chemicals and apparatus

Aniline (ANi) (99.5%) and *N*-methylaniline (NMA) (98.0%) monomers were purchased Aldrich Chemical Company. All monomers were vacuum-distilled and maintained under nitrogen atmosphere before use. ACN (99.0%) and TEABF<sub>4</sub> (99.0%) were purchased Sigma Aldrich and Fluka, respectively.

The conventional three-electrode system was used for all electrochemical experiments. PGE, platinum wire and silver wire were used as working electrode, counter electrode and pseudo reference electrode, respectively. PGE was Tombo leads with a diameter of 0.50 mm. The PGE was prepared by cutting the leads into 3 cm long sticks and 1 cm (area 0.16 cm<sup>2</sup>) was dipped in electrolyte. A Rotring Tikky pencil model was used as a holder for PGE. Electrical contact with the PGE was obtained by soldering a metallic wire to the metallic part of the holder. All electrodes were cleaned in ACN using ultrasonic bath (Bandelin Sonarex) and dried before each experiment. The all electrochemical measurements were carried out using A Gamry 3000 potentiostat/galvanostat/ZRA system (Wilmington, USA) and obtained datas were analyzed using Gamry CMS-300 (version 5.50b) framework/analysis software. All experiments were carried out at 25 °C and at open air atmosphere.

### 2.2. Electrochemical synthesis of PANi and PNMA

The PANi and the PNMA films were synthesized by electrochemical polymerizations of ANi and NMA on PGE from ANi and NMA containing ACN solutions using CV in the potential region between -0.20 V and +0.90 V versus Ag/AgCl at 50 mVs<sup>-1</sup> scan rate over 15 cycles. After electrochemical polymerizations PGE/PANi and PGE/PNMA was removed from the polymerization medium and rinsed with ACN to remove residues and dried in air.

### 2.3. Characterization of PANi and PNEA films

The surface morphologies of uncoated PGE, PGE/PANi and PGE/PNMA were investigated by means of SEM (Zeiss Ultra Plus Field Emission Scanning Electron Microscope).

Electrochemical characterizations of PANi and PNMA films were done in monomer free solution. CV method was used to research electro-kinetic behavior and electrochemical stability. To estimate electro-kinetic behavior, cyclic voltammetric curves were recorded in the potential of -0.20 V to +0.90 V at different scan rates ranged from 50 mVs<sup>-1</sup> to 350 mVs<sup>-1</sup>. To determine electrochemical stability, cyclic voltammetric curves were recorded in the same potential at scan rates of 50 mVs<sup>-1</sup> for 100 cycles. Doping types of the polymer films were determined via MS method. MS measurements were carried out in the potential range of -1.00 V to -0.20 V at 10<sup>4</sup> Hz.

#### 2.4. Determination of electrochemical storage properties

CV, potentiostatic EIS and RCP methods were used to determine electrochemical storage properties of the PGE/PANi and the PGE/PNMA. CV measurements were carried out using above procedure and  $C_{as}$  and  $C_{ms}$  values for different scan rates were calculated. The capacitance values were evaluated using the relation [27]:

$$C = \frac{i}{s} \quad (1)$$

where  $i$  is the current and  $s$  is scan rate.

Potentiostatic EIS properties were characterized at open circuit potential (OCP) in the frequency range  $10^5$  to  $10^{-2}$  Hz in monomer free solution of same electrolyte. The capacitance values at low frequency called as the low frequency capacitance ( $C_{LF}$ ) were evaluated using the relation [28]:

$$C_{LF} = -\frac{1}{\omega Z''} \quad (2)$$

where  $\omega (= 2\pi f)$  is the angular frequency and  $Z''$  is the imaginary part of the total complex impedance.

The  $C_{as}$  values of the electrodes are obtained by dividing the capacitance to area dipped in electrolyte. The  $C_{ms}$  values of the electrodes are obtained by dividing the capacitance to weight dipped in electrolyte [29,30].

Charge-discharge behaviors, also called as cycle durability of the PGE/PANi and the PGE/PNMA were investigated in monomer free solution using RCP method at  $\pm 2$  mA current for 1000 cycles. The specific power (SP,  $Wkg^{-1}$ ) and the specific energy (SE,  $Whkg^{-1}$ ) can be calculated from charge-discharge using the following relationships [31,32]:

$$SP = \frac{I\Delta E}{m} \quad (3)$$

$$SE = \frac{It\Delta E}{m} \quad (4)$$

where  $I$ ,  $t$  and  $m$  are the discharge current, discharge time and mass of electrode active materials, respectively.

### 3. RESULT AND DISCUSSION

#### 3.1. Electrochemical synthesis PANi and PNMA on PGE

Electrochemical synthesis can be carried out for the polymerization of ANi and its derivatives; (i) by controlling the anodic current (galvanostatic method), (ii) by holding the applied potential at

certain value (potentiostatic method) and (iii) by scanning the applied potential within a certain potential region (potentiodynamic method). The electro-oxidation of ANi and its derivatives by continuous cycling between the predetermined potentials produces an even polymeric film which firmly adheres on the electrode surface [33-36].

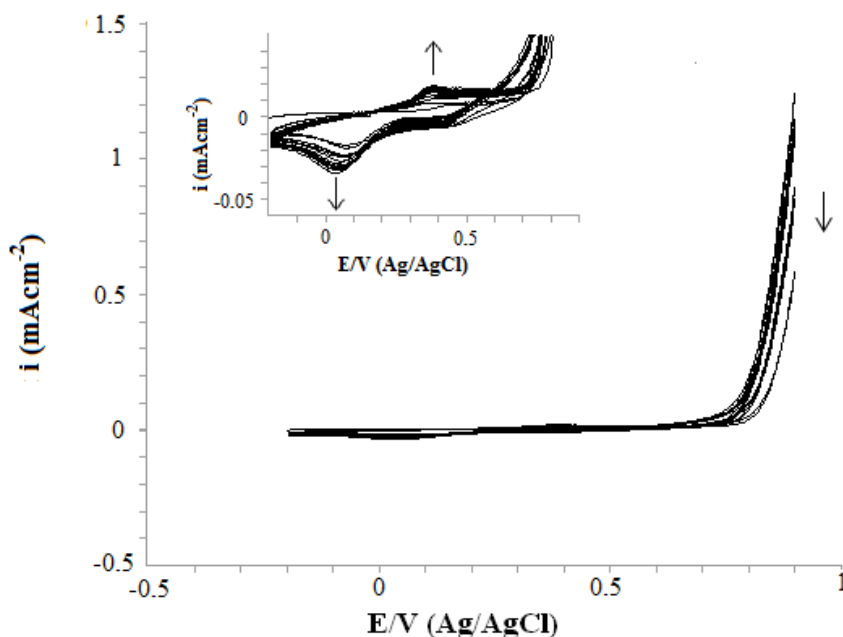


**Figure 1.** Cyclic voltammograms of the ACN solution containing 0.1 M TEABF<sub>4</sub> and 0.1 M ANi (scan rate: 50 mVs<sup>-1</sup>, cycles: 15).

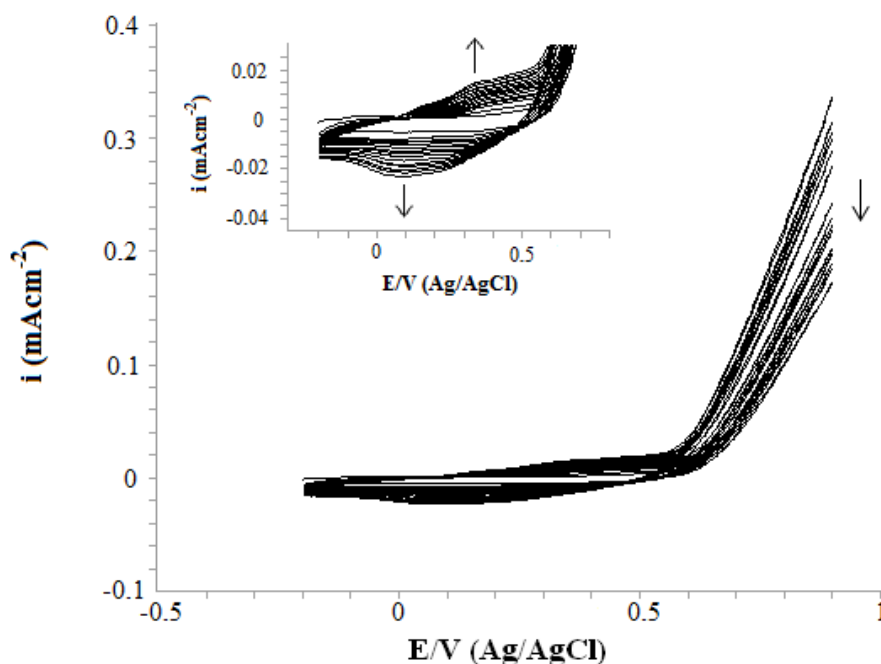


**Figure 2.** Cyclic voltammograms of the ACN solution containing 0.1 M TEABF<sub>4</sub> and 0.1 M NMA (scan rate: 50 mVs<sup>-1</sup>, cycles: 15).

PGE/PANi and PGE/PNMA were formed by loading PANi and PNMA on bare PGE using CV in 0.1 M monomer and 0.1 M TEABF<sub>4</sub> containing ACN solution, respectively. Fig. 1 and 2 show cyclic voltammograms of PANi and PNMA recorded between -0.20 V and +0.90 V, with a scan rate of 50 mVs<sup>-1</sup> for 15 cycles. For first scan, oxidation waves attributed to the oxidation of monomers appear starting at about +0.74 V and +0.60 V for ANi and NMA, respectively. The intensity of oxidation waves gradually decreases during subsequent scans. Starting with the second cycle, new one oxidation and one reduction peaks which belong to polymer formation were appeared. The oxidation peaks were observed at +0.36 V and +0.33 V and the reduction peaks were observed at +0.02 V and +0.08 V for PANi and PNMA, respectively. The peak current values associated with oxidation and reduction of PANi and PNMA increase with increasing scan number. This result indicates growth electroactive PANi and PNMA films on PGE surface [37, 38].

### 3.2. Surface morphologies of PGE/PANi and PGE/PNMA

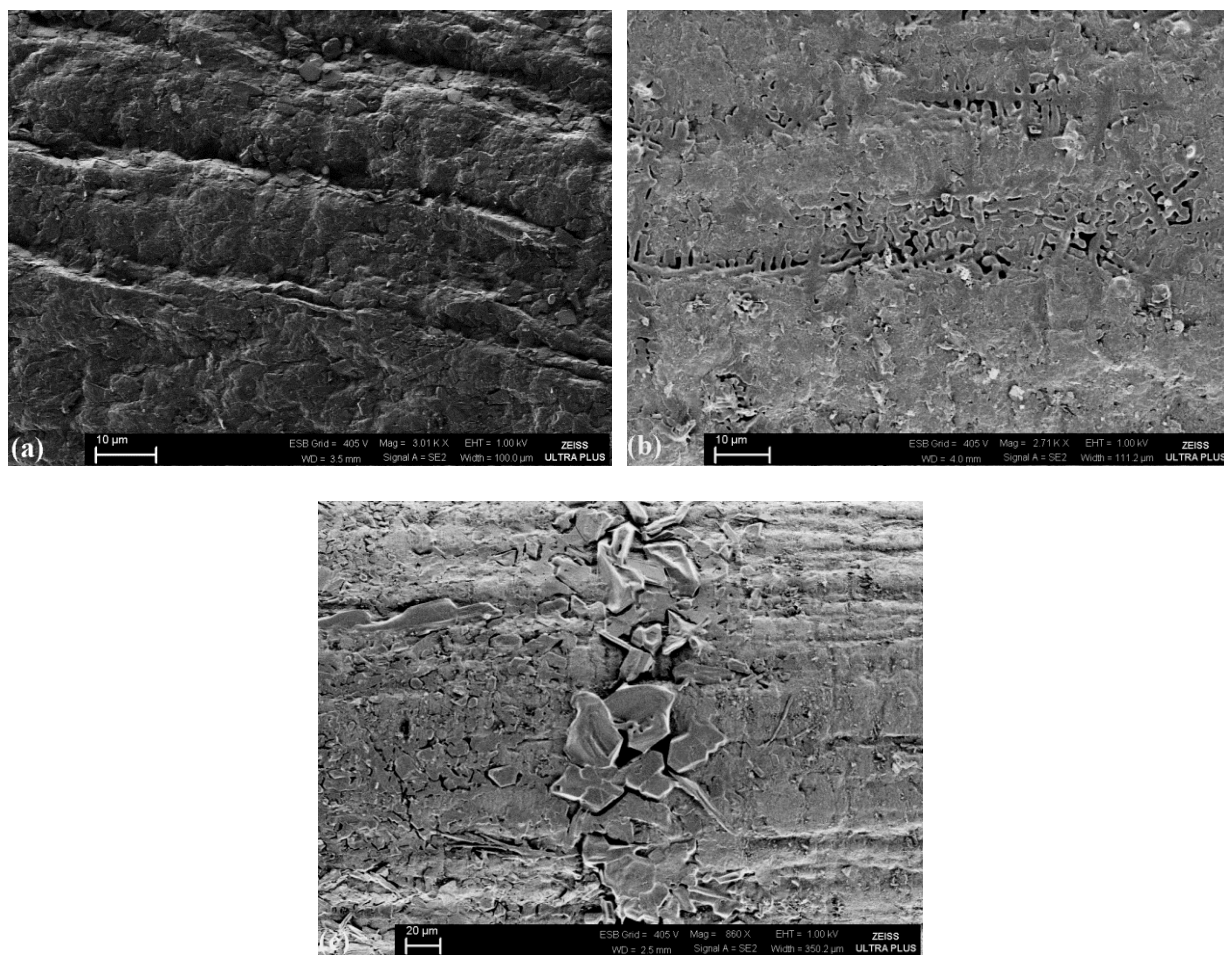


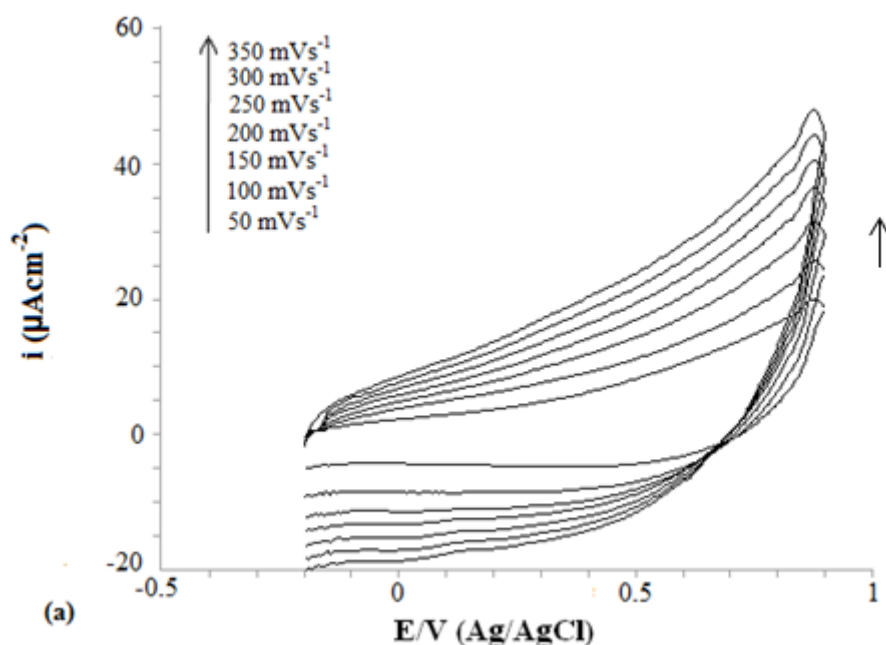
**Figure 3.** SEM images (a) uncoated PGE, (b) PGE/PANi and (c) PGE/PNMA.

The surface morphologies of uncoated PGE, PGE/PANi and PGE/PNMA were investigated by SEM and corresponding results were given in Fig. 3a-c. The SEM micrograph of uncoated PGE is also

shown in Fig. 3a for purpose comparison. As can be seen from this figure, the surface morphology of bare PGE is relatively uniform and rough and shows the presence of regularly ordered graphite layers. This rough and porous surface can be covered with the polymer film when the number of growth cycles is equal to fifteen (Fig. 3b-c). As shown in Fig. 3b, the irregular and heterogeneous masses belong to PANi can be seen on the surface of PGE/PANi. When the morphologies of PGE/PANi and PGE/PNMA are compared, it can be said that PGE/PNMA (Figure 3.c) has a similar structure with PGE/PANi. The PANi and PNMA films have a porous structure with flakes and this enables easy access for ions to access the electrode|electrolyte interface, which is a very important factor for the faradaic reactions [39]. This might enhance the electrochemical activity of polymer layers beneficial for the construction of high energy or high power energy sources.

### 3.3. Electrochemical characterization of PANi and PNMA

After electrochemical synthesis of PANi and PNMA films, their redox behaviors were investigated in monomer free solution by CV. Fig. 4a-b presents cyclic voltammograms of PANi and PNMA on PGE at different scan rates ranged from 50 to 350  $\text{mVs}^{-1}$  in the potential region between -0.20 V to +0.90 V. Fig. 5a-b shows anodic and cathodic peak current densities (obtained from Fig. 4a-b) associated with the oxidation and reduction of PANi and PNMA films as a function of the square root of scan rate and scan rate. As shown in Fig. 5a-b, linear relationships of anodic and cathodic peak current densities versus the square root of scan rate indicate that the electron transfer in both systems is essentially diffusion-controlled process [40]. A linear relationship between anodic and cathodic peak current densities and scan rate demonstrates that PANi and PNMA films are well adherent [41]. As shown, the slopes of the lines which are directly proportional with electroactivities of polymer films confirm that the PNMA film is more electroactive than PANi films [42].



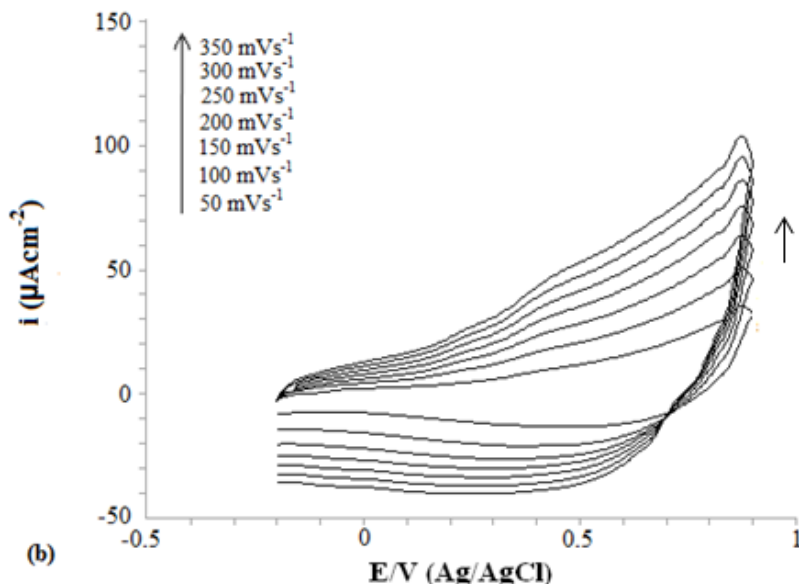


**Figure 4.** Cyclic voltammograms of (a) PANi and (b) PNMA films at different scan rates in ACN solution containing 0.1 M TEABF<sub>4</sub>.

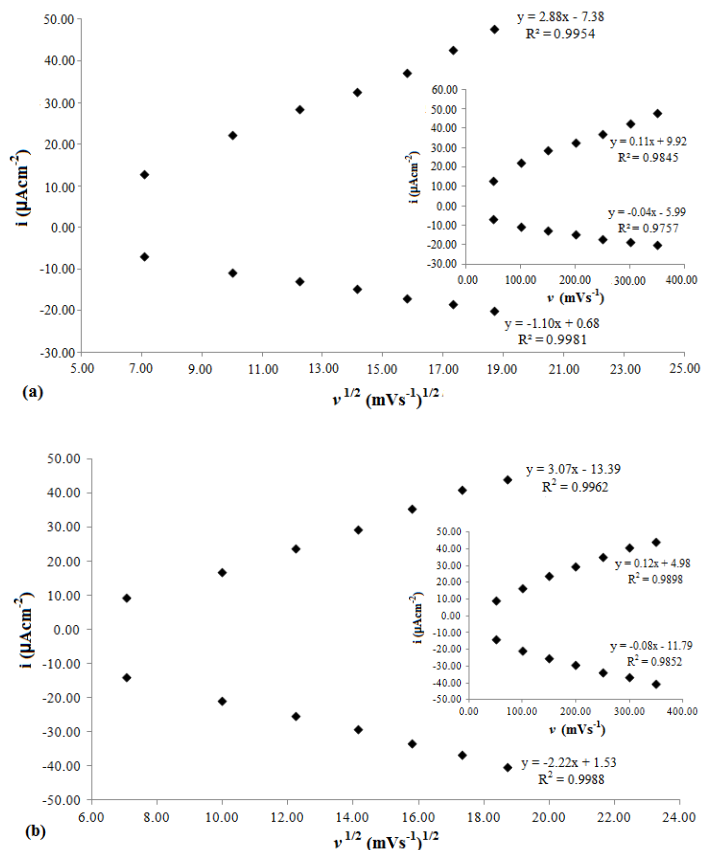


**Figure 5.** Plots of anodic and corresponding cathodic peak densities versus the square root of scan rate of the (a) PANi and (b) PNMA films up to 350 mVs<sup>-1</sup> in ACN solution containing 0.1 M TEABF<sub>4</sub> (Inset: plots of anodic and corresponding cathodic peak densities versus the scan rate of the (a) PANi and (b) PNMA films up to 350 mVs<sup>-1</sup> in ACN solution containing 0.1 M TEABF<sub>4</sub>).

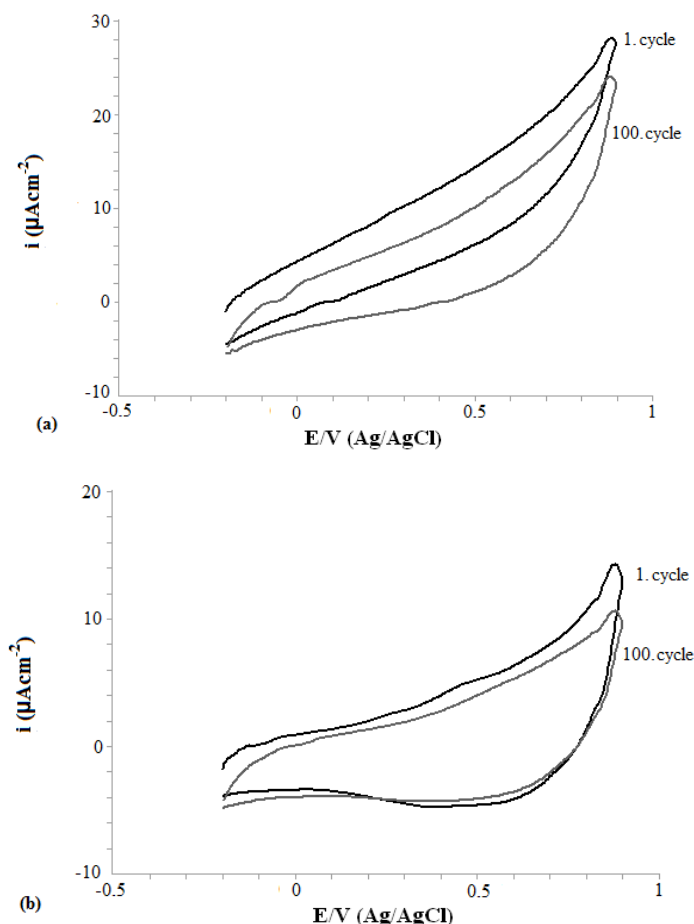


**Figure 6.** Stability tests for (a) PANi and (b) PNMA in ACN solution containing 0.1 M TEABF<sub>4</sub> (scan rate: 50 mVs<sup>-1</sup>, cycles: 100).

This result can be related to methyl groups combined with the nitrogen atoms in the PNMA polymer chain suppress the hydrolytic segmentation of the chain due to the electronic inductive effect and the methyl groups enhance the affinity between PNMA and dissolved organics [43].

The stability of conducting polymer in reduced and oxidized state is an important parameter for technological applications. The main reason that determines the lifetime of a conducting polymer is the chemical stability of the matrix itself. Fig. 6a-b shows the voltammograms for stability tests for PANi and PNMA films in monomer free solution at a scan rate of 50 mVs<sup>-1</sup> for 100 cycles in the potential range which polymer films were coated. Differences between initial and final anodic peak current density ( $\Delta I_{p_a}$ ) values were used to determine the stabilities of the films. If the PANi and PNMA films exhibit minimum decrease in  $I_{p_a}$  on repetitive cycling, the films are electrochemically most stable [44,45].  $\Delta I_{p_a}$  values of the obtained films calculated from Figure 6(a-c) are 2.44  $\mu\text{Acm}^{-2}$  and 0.56  $\mu\text{Acm}^{-2}$  for PANi and PNMA, respectively. It can be concluded that the PNMA film is more electrochemically stable than the PANi film.

Doping types of polymer films are determined the insertion of counter-ions coming from the electrolyte. While counter ion is anion or cation, doping types of polymer are p-type or n-type,

respectively [2, 46]. In our case, counter ion is tetrafluoroborate ( $\text{BF}_4^-$ ) anion coming from 0.1 M TEABF<sub>4</sub>/ACN electrolyte. This process have been seen from below reaction.



At the same time, MS behaviors of the PANi and PNMA coated on PGE give information about doping types of conducting polymers. MS plot is inverse square of capacitance, versus semiconductor electrode potential. Doping types of polymer can be determined by slope of the straight line of MS plots [47]. Negative slope shows p-type doping, positive slope shows n-type doping. MS experiments were performed in monomer free solution in the potential range of -1.00 V to -0.20 V at  $10^4$  Hz in monomer free solution and samples were equilibrated at an OCP for 600 s before each experiment and were given in Fig. 7a-b. As expected for a p-type doping, the MS slopes of the PANi and the PNMA films are negative (Fig. 7a-b) [48, 49].

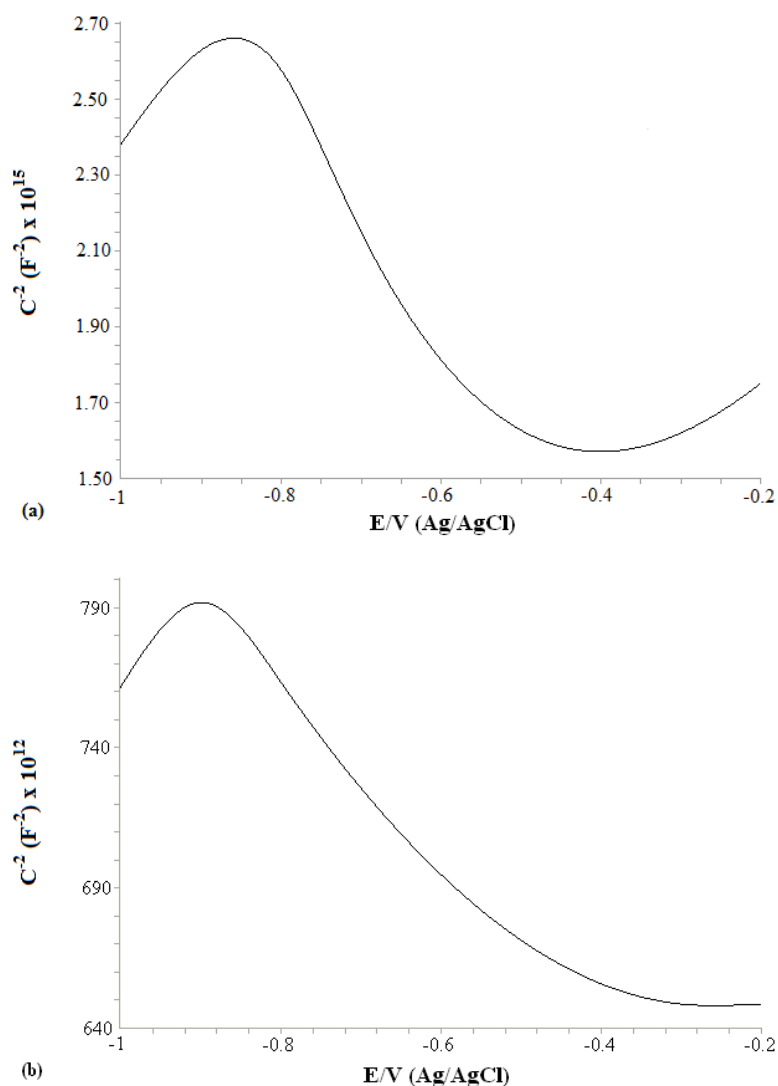


**Figure 7.** Mott-Schottky plots of (a) PANi and (b) PNMA films in ACN solution containing 0.1 M TEABF<sub>4</sub>.

### 3.4. Electrochemical storage properties of PGE/PANi and PGE/PNMA

The potential for using PGE/PANi and PGE/PNMA as electrode active materials for supercapacitor was investigated using CV, potentiostatic EIS and RCP techniques in monomer free solution. CV is considered an ideal tool for the characterization of electrochemical storage properties of any material. The cyclic voltammetric curves which were given in Fig. 4a-b, were used to evaluate effect of the scan rate on the specific capacitance. As can be seen from Fig. 4a-b, the area under curves was increased with the scan rate. This shows that the CV currents are directly proportional to the scan rates of CV, which demonstrates an ideal capacitive behavior [50-52]. The  $C_{as}$  and the  $C_{ms}$  values of the PGE/PANi and the PGE/PNMA calculated by Eq. (1) from Fig 4a-b were given in Table 1.

**Table 1.** Specific capacitance values of PGE/PANi and PGE/PNMA in ACN solution containing 0.1 M TEABF<sub>4</sub> at the different scan rates.

Scan Rate, mVs <sup>-1</sup>	PGE/PANi		PGE/PNMA	
	$C_{as}$ , $\mu\text{Fcm}^{-2}$	$C_{ms}$ , mFg <sup>-1</sup>	$C_{as}$ , $\mu\text{Fcm}^{-2}$	$C_{ms}$ , mFg <sup>-1</sup>
50	2920.75	35.21	3572.00	44.27
100	1403.77	16.92	1786.00	22.14
150	935.85	11.28	1190.00	14.76
200	733.33	8.84	893.08	11.06
250	561.51	6.77	714.47	8.85
300	467.92	5.64	595.39	7.73
350	401.07	4.83	510.33	6.32

It can be seen from Table 1 that the specific capacitance values decrease gradually with the increasing of the scan rate, this attributes to diffusion limitation of the electrolyte in pores of the PANi and the PNMA films. It is well known that the redox reactions on the PANi and the PNMA mainly attend by the doping-undoping counter ion (BF<sub>4</sub><sup>-</sup>) in the matrix of the polymer. Counter ions which are diffused from the electrolyte have access to almost all available spaces at low scan rates, leading to a complete insertion [53]. The decreasing trend of the specific capacitance can be related to parts of the surface of the electrode material are inaccessible at scan rates. Hence, the specific capacitance obtained at slow scan rates is thought to be closest to that of full utilization of the electrode material [51].

Potentiostatic EIS is a useful technique to monitor the electrochemical behavior of the electrodes and to characterize the frequency response of the electrochemical capacitance. PGE/PANi and PGE/PNMA were subjected to applied OCP and the impedance characteristics were recorded in the frequency range of 10<sup>5</sup> to 10<sup>-2</sup> Hz with potential amplitude of 10 mV in monomer free solution. OCP values of PGE/PANi and PGE/PNMA were determined as -0.10 V. Typical Nyquist diagrams for PGE/PANi and PGE/PNMA are given in Fig. 8. All the spectra are expected to exhibit a semicircle in the high frequency region and a linear portion at low frequency region for ideal supercapacitor behavior. The semicircle called as interfacial resistance which is combination of the charge transfer resistance and the double-layer capacitance at high frequencies is related to the faradaic process

occurred at the polymer film/electrolyte interface [54]. The linear curve at the low frequency region can be attributed to the diffusion controlled process in the electrolyte [55].

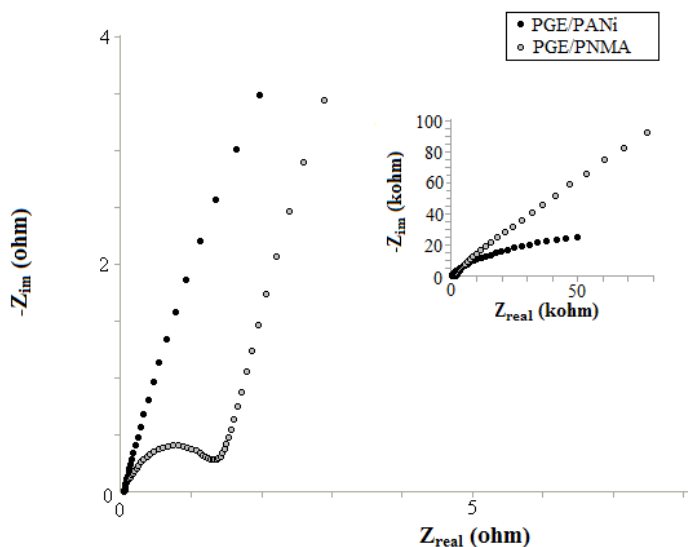


**Figure 8.** Enlarged version of low-resistance state of Nyquist plots of PGE/PANi and PGE/PNMA measured at OCP in ACN solution containing 0.1 M TEABF<sub>4</sub>. (Inset: Nyquist plots of PGE/PANi and PGE/PNMA measured at OCP in ACN solution containing 0.1 M TEABF<sub>4</sub>).

In our case, as can be seen from Fig. 8, Nyquist diagram of PGE/PANi has no semicircle at high frequency region, only a near vertical line is observed in the all range of scanned frequencies. It can be said that the PGE/PANi shows low interfacial resistance [56]. This behavior is close to an ideal electrical double layer capacitor and this can be explained that no any redox process occurred at -0.1 V [54,57]. However, a single semicircle and straight line can be observed for Nyquist diagram of the PGE/PNMA in the high and the low frequency regions, respectively. This result indicates that electrochemical storage property of the PGE/PNMA is based on both electrical double layer and faradaic process [58]. For supercapacitors, the majority of their capacitance is only available at low frequency, so attention should be paid to the data in this region [59]. Hence, we calculated the  $C_{LF}$ , the  $C_{ms}$  and the  $C_{as}$  values of electrodes using Eq. (2) from Bode plots belong to potentiostatic EIS measurements at  $10^{-2}$  Hz and gave in Table 2. It is clear that the specific capacitance values of PGE/PNMA are higher than PGE/PANi and these results have same trend when compared the results of CV.

**Table 2.** The low frequency capacitance and the specific capacitance value of PGE/PANi, and PGE/PNMA in ACN solution containing 0.1 M TEABF<sub>4</sub> using EIS.

Electrode	$C_{LF}$ , $\mu\text{F}$	$C_{as}$ , $\mu\text{Fcm}^{-2}$	$C_{ms}$ , $\text{mFg}^{-1}$
PGE/PANi	219.50	1380.50	16.64
PGE/PNMA	238.06	1487.88	18.57

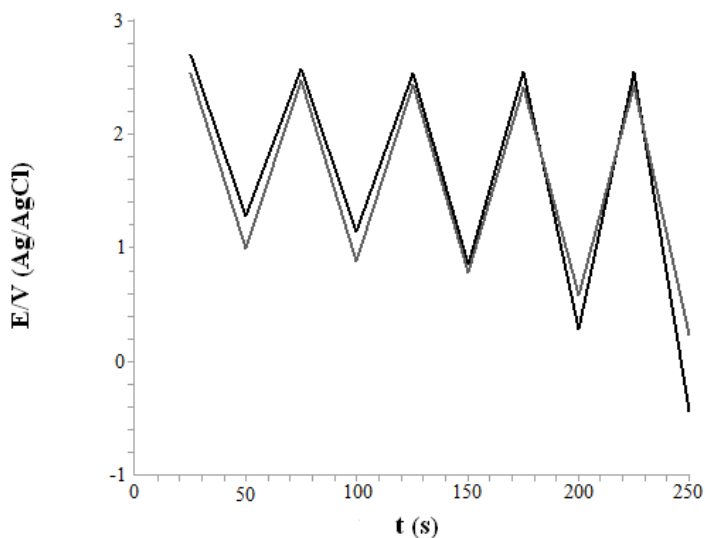


**Figure 9.** The first five cycles (—) and the last five cycles (---) of charge-discharge behavior of PGE/PNMA in ACN solution containing 0.1 M TEABF<sub>4</sub>.

The charge-discharge stability and reversibility of supercapacitor electrode active material, also called as cycle durability is important for its use in supercapacitor [60, 62]. For this purpose, the charge-discharge cycle stabilities of PGE/PANi and PGE/PNMA were investigated by means of RCP method. The charge-discharge process in monomer free solution was evaluated applying double current pulse during 25 s by 1000 consecutive cycles at  $\pm 2.00$  mA. Our result shows that PGE/PANi has a limited cycle life. After five cycles, PGE/PANi dissolved in monomer free solution and lost the charge-discharge cycle stability. Fig. 9 shows the first five cycles and the last five cycles of charge-discharge behaviors of PGE/PNMA in 1000 cycles of charge-discharge test. SP and SE values of the PGE/PNMA are calculated using Eq. 3 and 4 and are  $420.88 \text{ Wkg}^{-1}$  and  $10522.21 \text{ Whkg}^{-1}$ , respectively. On the other hand, potential of PGE/PNMA rose to 2.70 V. This indicates that PGE/PNMA can be suggested using for low voltage ( $< 10.00$  V) applications [46].

#### 4. CONCLUSIONS

In this study, we have been able to characterize PANi and PNMA coated PGE which is renewable and cheap pencil writing device and to investigate the utility of these electrodes as supercapacitor electrode active material. The PGE/PANi and the PGE/PNMA were electrochemically prepared in ACN solution containing 0.1 M TEABF<sub>4</sub> using CV. SEM results show that the structure of the PANi and the PNMA is similar. Electrochemical characterization which was done using CV and MS, were made on polymer coated PGE in monomer free solution. It was found that the PNMA film is more electrochemically stable than the PANi film and both films are p-doped state, according to CV and MS measurements, respectively. The electrochemical storage properties of the PGE/PANi and the PGE/PNMA were investigated by CV, EIS and charge-discharge tests. Results of CV and EIS methods

which were used to calculate the capacitance values of electrodes are same trend. The PGE/PNMA exhibits more higher specific capacitance than the PGE/PANi and the PGE/PNMA shows a better cycling stability than the PGE/PANi. On the other hand, PGE/PNMA can be suggested using for low voltage (< 10 V) applications including memory protection, video cameras, clock radios, UPS in alarm systems, smoke detectors and remote sensing [46].

#### ACKNOWLEDGEMENT

This work was supported by Eskişehir Osmangazi University Research Found (Project No: 2011/19010). The authors would like to thank to Associated Professor Müjdat Çağlar and Research Assistance Seval Aksoy for SEM.

#### References

1. B.E. Conway, *Electrochemical Supercapacitors, Scientific Fundamentals and Technological Applications*, Kluwer Academic/Plenum Publishers, New York, USA, 1999.
2. G.A. Snook, P. Kao and A.S. Best, *J. Power Sources* 196 (2011) 1.
3. Z.-Z. Zhu, G.-C. Wang, M.-Q. Sun, X.-W. Li and C.-Z. Li, *Electrochim. Acta* 56 (2011) 1366.
4. C. Du and N. Pan, *Nanotechnology* 17 (2006) 5314.
5. M.D. Stoller, S. Park, Y. Zhu, J. An and R.S. Ruoff, *Nano Lett.* 8 (2008) 3498.
6. K.H. An, W.S. Kim, Y.S. Park, J.-M. Moon, D.J. Bae, S.C. Lim, Y.S. Lee and Y.H. Lee, *Adv. Funct. Mater.* 11 (2001) 387.
7. D.W. Wang, F. Li, M. Liu, G.Q. Lu and H.M. Cheng, *Angew. Chem. Int. Ed.* 47 (2007) 373.
8. H. Zhang, G.P. Cao, Z.Y. Wang, Y.S. Yang, Z.J. Shi and Z.N. Gu, *Electrochem. Commun.* 10 (2008) 1056.
9. L.B. Kong, J.W. Lang, M. Liu, Y.C. Luo and L. Kang, *J. Power Sources* 194 (2009) 1194.
10. L.L. Zhang, R. Zhou and X.S. Zhao, *J. Mater. Chem.* 20 (2010) 5893.
11. W. Lu, L.T. Qu, K. Henry and L. Dai, *J. Power Sources* 189 (2009) 1270.
12. A.L.M. Reddy and S. Ramaprabhu, *J. Phys. Chem. C* 111 (2007) 7727.
13. X. Du, C.Y. Wang, M.M. Chen, Y. Jiao and J. Wang, *J. Phys. Chem. C* 113 (2009) 2643.
14. A. Rudge, I. Raistrick, S. Gottesfeld and J.P. Ferraris, *Electrochim. Acta* 39 (1994) 273.
15. K.S. Ryu, K.M. Kim, N.G. Park, Y.J. Park and S.H. Chang, *J. Power Sources* 103 (2002) 305.
16. K. Jurewicz, S. Delpheux, V. Bertagna, F. Beguin and E. Frackowiak, *J. Chem. Phys. Lett.* 347 (2001) 36.
17. B. Muthulakshmi, D. Kalpana, S. Pitchumani and N.G. Renganathan, *J. Power Sources* 158 (2006) 1533.
18. Q. Wang, J.-I. Li, F. Gao, W.-S. Li, K.-Z. Wu and X.-D. Wang, *New Carbon Materials* 23 (2008) 275.
19. R.K. Sharma, H.S. Oh, Y.G. Shul and H.S. Kim, *J Power Sources* 173 (2007) 1024.
20. S. Devaraj and N. Munichandraiah, *J. Electrochem. Soc.* 154 (2007) A80.
21. T. Sotomura, H. Uemachi, K. Takeyama, K. Naoi and N. Oyama, *Electrochim. Acta* 37 (1992) 1851.
22. E.M. Genies and S. Picart, *Synth. Met.* 69 (1995) 165.
23. K. Naoi, K.-I. Kawase, M. Mori and M. Komiyama, *J. Electrochem. Soc.* 144 (1997) L173.
24. C.-C. Hu and C.-H. Chu, *Mater. Chem. Phys.* 65 (2000) 329.
25. E.T. Kang, K.G. Neoh and K.L. Tan, *Handbook of Organic Conductive Molecules and Polymers*, Wiley, New York, USA, 1997.

26. Y.-Y. Horng, Y.-C. Lu, Y.-K. Hsu, C.-C. Chen, L.-C. Chen and K.-H. Chen, *J. Power Sources* 195 (2010) 4418.
27. B. He, Y. Zhou, W. Zhou, B. Dong and H. Li, *Mater. Sci. Eng.* 374 (2004) 322.
28. J. Wang, Y. Xu, X. Chen and X. Du, *J. Power Sources* 163 (2007) 1120.
29. U.M. Patil, S.B. Kulkarni, V.S. Jamadade and C.D. Lokhande, *J. Alloy. Compd.* 509 (2011) 1677.
30. Y. Hu, H. Zhu, J. Wang, and Z. Chen, *J. Alloy. Compd.* 509 (2011) 10234.
31. V. Gupta and N. Muira, *Electrochem. Solid-State Lett.* 8 (2005) A630.
32. H. Yu, J. Wu, L. Fan, Y. Lin, K. Xu, Z. Tang, C. Cheng, S. Tang, J. Lin, M. Huang and Z. Lan, *J. Power Sources* 198 (2012) 402.
33. E.M. Genies, A.A. Syed and C. Tsintavis, *Mol. Cryst. Liq. Cryst.* 121 (1985) 181.
34. E.M. Genies and C. Tsintavis, *J. Electroanal. Chem.* 195 (1985) 109.
35. S. Bhadra, D. Khastgir, N.K. Singha and J.H. Lee, *Prog. Poly. Sci.* 34 (2009) 783.
36. D.D. Borole, U.R. Kapadi, P.P. Mahulikar and D.G. Hundiwale, *Mater. Lett.* 60 (2006) 2447.
37. B. Duran, M.C. Turhan, G. Bereket and A.S. Saraç, *Electrochim. Acta* 55 (2009) 104.
38. G. Bereket, E. Hür, Y. Şahin, *Appl. Surf. Sci.* 252 (2005) 1233.
39. D.P. Dubal, V.J. Fulari and C.D. Lokhande, *Micropor. Mesopor. Mater.* 151 (2012) 511.
40. G. Feng, Y. Xiong, H. Wang and Y. Yang, *Electrochim. Acta* 53 (2008) 8253.
41. F.Ç. Cebeci, H. Geyik, E. Sezer and A.S. Saraç, *J. Electroanal. Chem.* 610 (2007) 113.
42. L. Shadi, H. Gheybi, A.A. Entezami and K.D. Safa, *J. Appl. Polym. Sci.* 124 (2012) 2118.
43. J. Yano, M. Kokura and K. Ogura, *J. Appl. Electrochem.* 24 (1994) 1164.
44. A.S. Saraç, E. Doğru, M. Ateş and E.A. Parlak, *Turk. J. Chem.* 30 (2006) 401.
45. B. Duran, G. Bereket, M.C. Turhan and S. Virtanen, *Thin Solid Films* 519 (2011) 5868.
46. M. Mastragostino, C. Arbizzani and F. Soavi, *J. Power Sources* 97-98 (2001) 812.
47. A.S. Bondarenko and G.A. Ragoisha, *J. Solid State Electrochem.* 9 (2005) 845.
48. K.L. Levine, D.E. Tallman and G.P. Bierwagen, *J. Mater. Processing Technol.* 199 (2008) 321.
49. A. Fikus, U. Rammelt and W. Plieth, *Electrochim. Acta* 44 (1999) 2025.
50. D.P. Dubal, W.B. Kim and C.D. Lokhande, *J. Phys. Chem. Solids* 73 (2012) 18.
51. T.P. Gujar, W. Kim, I. Puspitasari, K.D. Jung and O.-S. Joo, *Int. J. Electrochem. Sci.* 2 (2007) 666.
52. U.M. Patil, R.R. Salunkhe, K.V. Gurav and C.D. Lokhande, *Appl. Surf. Sci.* 255 (2008) 2603.
53. M. Jin, G. Han, Y. Chang, H. Zhao and H. Zhang, *Electrochim. Acta* 56 (2011) 9838.
54. H. Heli, H. Yadegari and A. Jabbari, *Mater. Chem. Phys.* 134 (2012) 21.
55. J. Gamby, P.L. Taberna, P. Simon, J.F. Fauvarque and M. Chesneau, *J. Power Sources* 101 (2001) 109.
56. A. Laforgue, *J. Power Sources* 196 (2011) 559.
57. R.K. Sharma and L. Zhai, *Electrochim. Acta* 54 (2009) 7148.
58. C.-C. Hu and C.-H. Chu, *J. Electroanal. Chem.* 503 (2001) 105.
59. B.P. Bakhmatyuk, B.Y. Venhryn, I.I. Grygorchak and M.M. Micov, *J. Power Sources* 180 (2008) 890.
60. V.S. Jamadade, V.J. Fulari and C.D. Lokhande, *J. Alloys Compd.* 509 (2011) 6257.
61. J. Li, E.H. Liu, W. Li, X.Y. Meng and S.T. Tan, *J. Alloys Compd.* 478 (2009) 371.